JOURNAL OF CATALYSIS 133, 527–543 (1992)

On the Nature of the Active Sites for Ethylene Hydrogenation in Metal-Free Zeolites

JUNICHI KANAI,[1] JOHAN A. MARTENS, AND PETER A. JACOBS

Centrum voor Oppervlaktechemie en Katalyse, Department of Interface Chemistry, Katholieke Universiteit Leuven, Kardinaal Mercierlaan 92, B-3001 Leuven, Belgium

Received July 27, 1990; revised May 2, 1991

The hydrogenation of ethylene has been studied over acid faujasites, mordenite, and ZSM-5 zeolites at reaction temperatures varying between 623 and 723 K and a hydrogen pressure of 1 MPa. The active sites responsible for the hydrogenation of ethylene change from sodium cations to Brønsted acid sites when the reaction temperature is increased from 623 K to 723 K. The change of the active sites is reflected in the temperature dependence of the ethane yield. It is suggested that the hydrogenation of ethylene on Brønsted acid sites requires only a single site and occurs via a pentacoordinated carbonium ion mechanism. Different behavior of acid sites in various zeolites is attributed to topological differences.

INTRODUCTION

In the past, several hypotheses on the nature of the sites responsible for the activation of hydrogen in metal-free zeolites have been advanced. Heylen *et al.* (*1*) studied the H_2–D_2 equilibration over Y zeolites at a temperature of 673 K and a pressure of 5 kPa and found that the activity increased with the iron impurity content of the zeolite. Later, it was confirmed that the same impurities were also responsible for the dehydrogenation of isopropanol over X and Y zeolites at reaction temperatures around 393 K and using a hydrogen pressure of 0.1 MPa (*2*). Gnep *et al.* (*3*) studied the disproportionation of toluene over mordenites at 723 K and hydrogen pressures of 1.5 MPa. They found that under such reaction conditions, metal-free mordenites were capable of activating hydrogen. They proposed either strong acid centers or impurity elements such as iron as active sites.

Minachev *et al.* (*4, 5*) studied the hydrogenation of aromatic and olefinic hydrocarbons over cationic forms of zeolites. The reaction temperatures were in the range from 413 to 573 K and the pressure from 3 to 6 MPa. The same authors reported that the hydrogenation activity of a zeolite increased with its cation content and concluded that cations were responsible for the hydrogenation activity (*4, 5*).

Recently, Sano *et al.* (*6*) found that HZSM-5 catalyzes the hydrogenation of ethylene at a pressure of 4 MPa in the temperature range from 623 to 823 K. In another study (*7*) it was reported that HZSM-5 and H-mordenite show a high catalytic activity in the hydrocracking of benzene at temperatures of 573 to 873 K and a pressure of 4 MPa, and that on the contrary, H–Y, HZSM-34, and silica–alumina show only a very low activity. Since the activity of HZSM-5 and H-mordenite increased with decreasing Si/Al ratio of the zeolite, irrespective of the content of impurity iron, it was proposed that strong acid sites are responsible for the hydrocracking of benzene (*7*).

Thus, essentially three different types of sites have been proposed in the literature for the activation of hydrogen in metal-free zeolites, viz. iron impurities, alkali metal

[1] On leave from Idemitsu Kosan Co. Ltd., Japan.

0021-9517/92 $3.00

cations, and Brønsted acid sites. In this work, the hydrogenation of ethylene has been studied over a series of faujasite, mordenite, and ZSM-5 zeolites modified in such a way that systematic variations in the relative concentrations of the suggested active sites existed. As can be derived from pertinent literature data, different hydrogenation mechanisms may be operative on the same catalyst, their contribution depending largely on reaction conditions such as temperature and hydrogen partial pressure.

EXPERIMENTAL

Materials

The parent samples were a NaY from Union Carbide Corp., an ultrastable Y zeolite (USY) from Zeocat (type ZF 510), a H-mordenite (type Zeolon-100H) from Norton, high alumina–ZSM-5 synthesized according to a template-free method (*8*), and siliceous ZSM-5 synthesized using tetrapropylammonium (TPA) (*9*). Figures in brackets in the sample notation refer to Si/Al framework ratios of the samples as determined with ^{29}Si and ^{27}Al MAS NMR. They are a measure of the Brønsted site concentration as they refer only to lattice Al. This does not hold for USY(4), which contains extra-framework Al and for NaUSY(8), which contains residual Na. In the case of HNaY, these figures refer to degrees of NH_4^+ or H^+ exchange. The parent USY(8) sample from Zeocat does not contain extra-framework Al. From the amount of framework Al and the residual sodium, the proton content of the samples was determined.

The parent zeolite samples were modified according to the procedures outlined in Table 1.

The zeolite powder was pelletized without binder, crushed, and sieved. Particles with diameters from 0.25 to 0.50 mm were used in the catalytic experiments. The catalysts were stored in water-saturated air.

The crystallinity, chemical composition, and BET surface area of the catalysts are given in Table 2.

Catalytic Experiments

Catalytic reactions were carried out using a tubular quartz reactor with an internal diameter of 4 mm, mounted inside a stainless-steel tube. Those parts of the stainless-steel tube that are exposed to the reactant gas were kept at a temperature below 323 K. In a blank experiment the quartz reactor was packed with quartz pellets and quartz wool. No catalytic activity was found at a reaction temperature of 723 K.

The catalysts were activated *in situ* in the reactor under flowing oxygen at a pressure of 0.1 MPa using a final temperature of 723 K for 1.5 h. For the experiments performed at 723 K, the reactor was flushed with nitrogen and held for 20 min at a pressure of 2 MPa in a nitrogen–hydrogen mixture containing 50 vol% of hydrogen. For the experiments performed at 623 K, the reactor was cooled under nitrogen after the oxygen treatment. The volumetric composition of the reactant gas mixture was 50% of hydrogen, 49% of nitrogen, and 1% of ethylene. The amount of catalyst was 200 mg and the WHSV of ethylene was 1.0 h^{-1}.

Analysis of the reaction products was carried out by on-line gas chromatography (GC) using a 50-m OV-101 glass capillary column. The transfer line from the reactor to the GC was heated at 373 K to prevent condensation of the reaction products. The mass balance in all experiments was higher than 90 wt%.

A reactant gas mixture containing deuterium, nitrogen, and ethylene in a 50 : 49 : 1 volume ratio was used for the deuterium experiment. Deuterium (99.8%) was obtained from Alphagaz Co. and used with no further purification. The reaction products were collected in a vessel for 15 min and analyzed by GC/MS (Hewlett Packard, 5988A). A 100-m OV-101 glass capillary column was used in the GC/MS instrument. The coke content of the used catalysts was measured gravimetrically using a Setaram thermobalance. The catalysts were heated to 1273 K under a flow of air and the weight

TABLE 1

Preparation Procedures of Zeolite Catalysts

Catalyst notation	Preparation method
HNaY-19	NaY, as-received, sodium deficient
HNaY-71	NaY, exchanged at reflux with excess NH_4^+
HNaY-91	NaY, repeated exchange with excess NH_4^+ at reflux
USY(4)	steaming of NH_4NaY-91 at 1023 K
USY(8)	USY, as-received
USY(11)	USY(8) refluxed with a 0.1 *N* HCl solution
USY(27)	USY(8) refluxed with a 0.3 *N* HCl solution
USY(47)	USY(8) refluxed with a 0.5 *N* HCl solution
NaUSY(8)	USY(8), back-exchanged with Na^+
HM(8)	H-mordenite, as-received
HM(11)	M(8) refluxed with a 1.0 *N* HCl solution
HM(12)	M(8) refluxed with a 4.0 *N* HCl solution
HM(23)	M(8) self-steamed at 923 K and refluxed with a 4.0 *N* HCl solution
HM(49)	M(23) self-steamed at 923 K and refluxed with a 4.0 *N* HCl solution
HZSM-5(13)	As-synthesized sample exchanged with NH_4^+ (template-free synthesis)
HZSM-5(39)	As-synthesized sample calcined at 823 K, and exchanged with NH_4^+ (TPA-type synthesis)
HZSM-5(60)	As-synthesized sample calcined at 823 K, and exchanged with NH_4^+ (TPA-type synthesis)

loss was determined between 673 and 873 K.

RESULTS AND DISCUSSION

Hydrogenation Activity on HNaY Zeolite

The hydrogenation of ethylene over the HNaY catalysts was performed at reaction temperatures of 623 and 723 K. In all experiments with HNaY zeolites, the main reaction product was ethane and the yield of methane and C_3 to C_5 hydrocarbons was below 10 wt%. The variation of the ethane yield at 623 and 723 K with time-on-stream is given in Figs. 1 and 2, respectively. At a reaction temperature of 623 K, the ethane yield at a given time-on-stream increases among the catalysts in the following order:

$$\text{HNaY-19} > \text{HNaY-71} > \text{HNaY-91},$$

suggesting that a relation exists between catalytic activity and the Na content of the samples. At a reaction temperature of 723 K, an opposite initial activity sequence is encountered, viz.

$$\text{HNaY-19} < \text{HNaY-71} < \text{HNaY-91}.$$

Now the relation between catalytic activity and proton content of the catalysts is obvi-

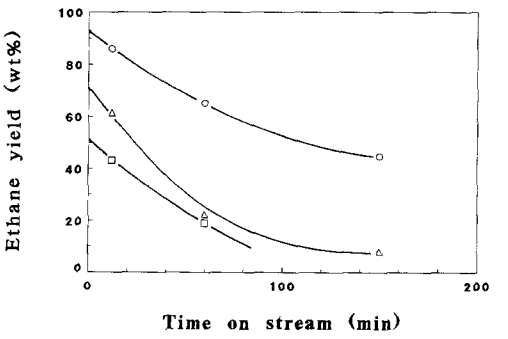

FIG. 1. Ethane yield in the hydrogenation of ethylene as a function of time-on-stream at 623 K and 1 MPa of H_2: (○) HNaY-19, (△) HNaY-71, and (□) HNaY-91.

TABLE 2

Catalyst Properties

Catalyst	Crystallinity (%)	a_0 (nm)	Si/Al[a]	Si/Al[b]	Framework Al[b] (mmol/g)	Na (mmol/g)	Fe (ppm)	Surface area ($m^2\ g^{-1}$)
HNaY-19	100[c]	2.478	2.5	2.8	4.11	3.33	760	597
HNaY-71	100	2.477	2.5	2.7	4.44	1.30	760	591
HNaY-91	100			2.6	4.56	0.39	740	603
USY(4)	100	2.457	4.5	3.3	3.04[a]	0.04	280	572
USY(8)	100	2.443	8.5	8.3[e]	1.79	0.06	1150	583
USY(11)	99	2.437	13.3	11.0[e]	1.38	0.02	1010	593
USY(27)	94	2.432	21.9	26.9[e]	0.60	0.02	840	625
USY(47)	54	2.426	69.5	47.3[e]	0.34	0.02	460	600
NaUSY(8)				7.6	1.90	0.70	1080	
HM(8)	100[d]			7.6[e]	1.94	0.14	1000	382
HM(11)	100			11.1[e]	1.37	0.06	280	401
HM(12)	100			11.5[e]	1.34	0.03	190	406
HM(23)	100			23.3[e]	0.69	0.01	80	425
HM(49)	100			49.4[e]	0.33	0.01	90	
HZSM-5(13)				13.5[e]	1.15	0.002		
HZSM-5(39)				39.2[e]	0.41	0.01	290	338
HZSM-5(60)				60.0[e]	0.27			

[a] Calculated from a_0 values according to: $N_{Al} = 107.1\ (a_0 = 22.24)$

[b] Determined by chemical analysis.

[c] The crystallinity of HNaY-19 was assumed to be 100% in Y-type zeolites.

[d] The crystallinity of M(8) was assumed to be 100% in mordenites.

[e] Identical to values determined by ^{29}Si and ^{27}Al MAS NMR.

ous. Consequently, as the three catalysts contain about the same content of iron (Table 2) it seems that at 623 K, the activity could be due to sodium cations, whereas at 723 K, protons could be the active sites.

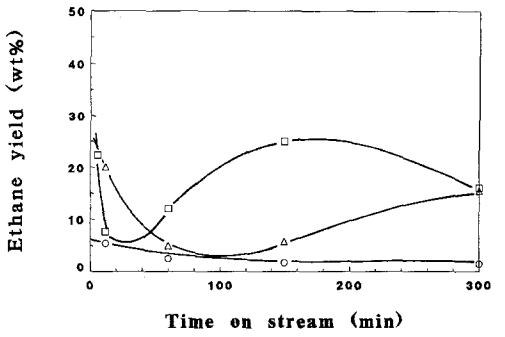

FIG. 2. Ethane yield in the hydrogenation of ethylene as a function of time-on-stream at 723 K and 1 MPa of H_2: (○) HNaY-19, (△) HNaY-71, and (□) HNaY-91.

The existence of two different sites and mechanisms is further substantiated by the temperature dependence of the initial ethane yields. In the temperature range from 600 to 750 K, a minimum is always observed (see also Fig. 14). Arrhenius plots of the corresponding rate data would reveal apparent activation energies that are negative at lower temperatures, followed by positive ones at higher temperatures. Negative apparent activation energies have been reported for the hydrogenation of ethylene over nickel metal at high reaction temperatures (*10*). These data confirm that two reaction mechanisms are operative and are not in contradiction with the earlier conclusion that in HNaY zeolites the active sites change from sodium cations to protons in the temperature range between 623 and 723 K.

In principle, two reaction mechanisms are

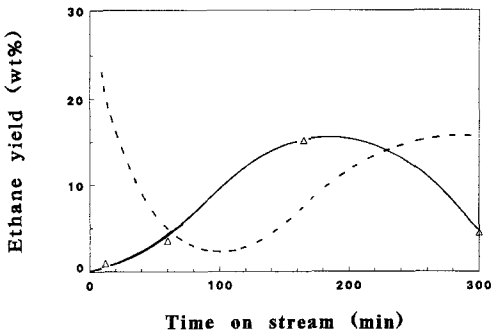

FIG. 3. Ethane yield from ethylene in absence of hydrogen gas as a function of time-on-stream over HNaY-71, 723 K, WHSV of C_2H_4 = 1 h^{-1}; N_2:C_2H_4 = 99:1. The dashed line corresponds to the same experiment in the presence of hydrogen.

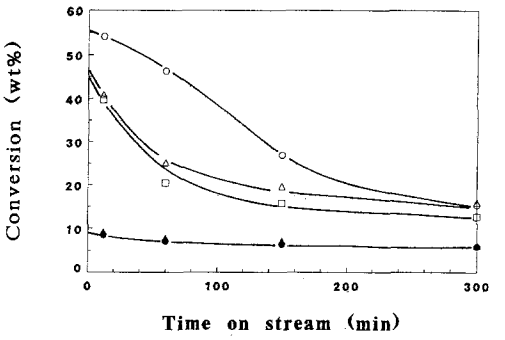

FIG. 4. Conversion of ethylene at 723 K in the presence of 1 MPa of hydrogen as a function of time-on-stream: (○) USY(4), (△) USY(8), (□) USY(11), (●) USY(27), (▲) USY(47).

possible for the formation of ethane on Brønsted acid sites, (i) hydrogen transfer from coke to ethylene and (ii) direct hydrogenation of ethylene through catalytic hydrogen activation.

HNaY-71 and HNaY-91 samples deactivate rapidly in the presence of hydrogen at 723 K (Fig. 2). Later, the ethane yield increases again, especially for the HNaY-91 sample (Fig. 2). After a time-on-stream of 5 h, the used HNaY-19 sample had no coke, while the coke content of used HNaY-71 and HNaY-91 was 9.8 and 10.8 wt%, respectively.

In order to discriminate between true hydrogenation and hydrogen transfer, ethylene was converted in the absence of hydrogen over HNaY-71 at 723 K. Initially, the ethane yield was very low but increased during the first 160 min on stream (Fig. 3). After 5 h of operation, the coke content of the catalyst was 27.8 wt%.

In contrast, in the presence of hydrogen the initial ethane yield is high (Fig. 2), which could reflect the hydrogenation activity of Brønsted acid sites. The ethylene hydrogenation activity of the Brønsted acid sites disappears rapidly (Fig. 2), probably as a result of the deposition of coke precursor molecules. At a later stage of the reaction in Fig. 2, hydrogen transfer from coke to ethylene is responsible for increased ethane yield.

Hydrogenation Activity on Ultrastable Y Zeolites

The hydrogenation of ethylene over the USY catalysts was also performed at a reaction temperature of 723 K in otherwise identical conditions. The change with time-on-stream of the ethylene conversion is given in Fig. 4. The activity of USY is lower for samples with higher Si/Al ratio, suggesting that the concentration of Brønsted acid sites is proportional to the reaction rate. The corresponding selectivity for ethane, C_3 to C_5 alkanes, and methane is shown in Figs. 5,

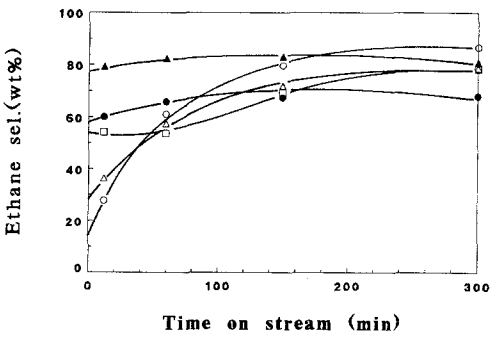

FIG. 5. Selectivity for ethane as a function of time-on-stream at 723 K: (○) USY(4), (△) USY(8), (□) USY(11), (●) USY(27), (▲) USY(47).

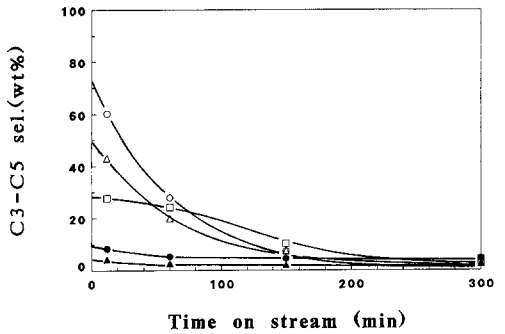

FIG. 6. Selectivity for C3 to C5 alkanes as a function of time-on-stream at 723 K: (○) USY(4), (△) USY(8), (□) USY(11), (●) USY(27), (▲) USY(47).

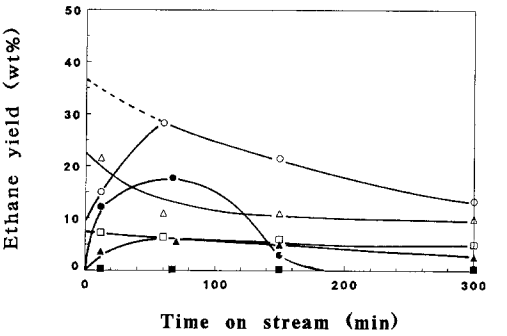

FIG. 8. Effect of the reaction atmosphere on the ethane yield from ethylene at 723 K: (○, ●) USY(4); (△, ▲) USY(11): (□, ■) USY(47). Open symbols refer to the molar ratio $H_2 : N_2 : C_2H_4 = 50 : 49 : 1$; solid symbols refer to $N_2 : C_2H_4 = 99 : 1$.

6, and 7, respectively. The most siliceous sample, USY(47), exhibits the highest initial ethane selectivity. When the Si–Al ratio of the catalyst is lower, the initial ethane selectivity decreases, in contrast to what is observed for the selectivity for C_3 to C_5 products (Figs. 5 and 6). C_3^+ hydrocarbons should stem from oligomerization of ethylene and subsequent cracking of the oligomers.

The selectivity for methane decreases systematically when the Si/Al ratio of the catalyst is increased from 8 to 47 (Fig. 7). The more aluminous USY(4) catalyst exhibits a low methane selectivity (Fig. 7) and, therefore, violates this trend.

In order to discriminate between true hydrogenation and hydrogen transfer, ethylene was converted in the absence of hydrogen over USY(4), USY(11), and USY(47). The initial yield of ethane on USY(47) is negligible (Fig. 8) compared to that observed in the presence of hydrogen. On USY(4) the yield of ethane in the absence of hydrogen is important (Fig. 8), and consequently, ethane should for a large extent come from hydrogen transfer reactions. With USY(11), an intermediate situation occurs in which both hydrogenation and hydrogen transfer are important (Fig. 8).

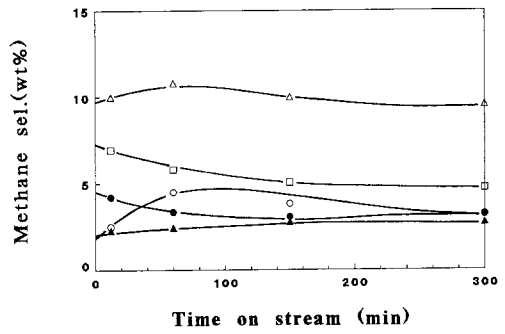

FIG. 7. Selectivity for methane as a function of time-on-stream at 723 K: (○) USY(4), (△) USY(8), (□) USY(11), (●) USY(27), (▲) USY(47).

The yield of C_3 to C_5 alkanes on USY(4) and USY(11) in the presence and absence of hydrogen are compared in Fig. 9. The initial yield of C_3^+ saturates does not depend on the presence of hydrogen, indicating that saturated C_3^+ products are formed through hydrogen transfer reactions. Preferential hydrogen transfer to olefins larger than ethylene can be explained by the higher stability of larger alkylcarbenium ions.

A parameter of the relative importance of true hydrogenation compared to hydrogen transfer can be derived from the molar composition of the reaction products using the equations

$$C_2^{2-} + H_2 \rightarrow C_2$$

$$xC_2^{2-} \rightarrow C_3^{2-} \text{ to } C_5^{2-}$$

$$C_3^{2-} \text{ to } C_5^{2-} \rightarrow \text{coke} + C_3 \text{ to } C_5.$$

This parameter can be defined as

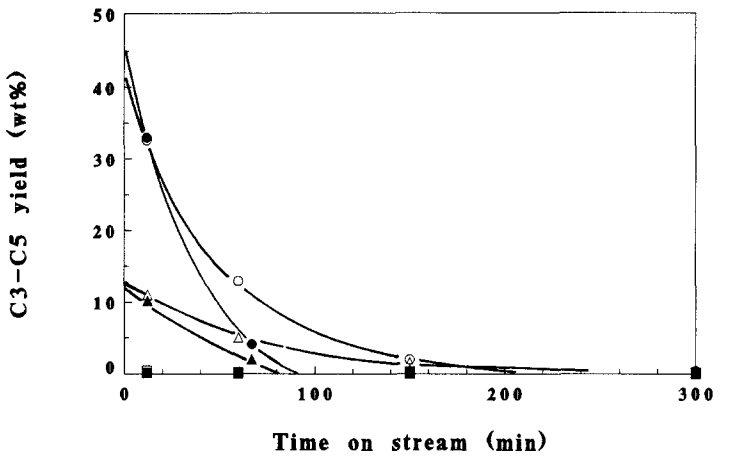

FIG. 9. Effect of the reaction atmosphere on the yield of C_3 to C_5 alkanes at 723 K: (○, ●) USY(4); (△, ▲) USY(11): (□, ■) USY(47). Open symbols, $H_2 : N_2 : C_2H_4 = 50 : 49 : 1$; solid symbols, $N_2 : C_2H_4 = 99 : 1$.

$$k_1/k_2 = \frac{\text{(mol of ethane)} \times \text{(mol of } C_3 \text{ to } C_5 \text{ alkenes)}}{\text{(mol of ethylene)} \times \text{(mol of } C_3 \text{ to } C_5 \text{ alkanes)}}.$$

Indeed, as ethane and the C_3 to C_5 alkanes stem mainly from ethylene hydrogenation and hydrogen transfer from coke to C_3 to C_5 alkenes, respectively, this parameter is a measure of the relative importance of true hydrogenation compared with hydrogen transfer. For the different catalysts initial k_1/k_2 ratios were determined by extrapolation to zero time-on-stream (Fig. 10). The initial k_1/k_2 values of USY zeolite decrease with increasing proton content, indicating that hydrogen transfer compared to true hydrogenation becomes more difficult when the acid density of the zeolite decreases. It cannot be concluded from the data that the catalytic activity per site is constant, as k_1 and k_2 are not always rates measured in differential conditions. However, as Pine *et al.* (*11*) and Guisnet *et al.* (*12, 13*) proposed that bimolecular reactions become more difficult than monomolecular reactions when the acid density decreases, it is suggested that in the hydrogenation of ethylene only a single acid site is involved, whereas hydrogen transfer requires more than one active site.

The active sites on USY(4) initially produce C_3 to C_5 alkanes in a selective way (Fig. 6), but their selectivity changes toward ethane formation with time-on-stream. Thus after partial coverage of the acid sites with coke, ethane is produced on the remaining isolated acid sites. Therefore, the initial ethane yield should be a measure of the hydrogenation activity. In Figs. 11 and 12, this initial ethane yield is plotted against the proton and iron content in the HNaY and USY catalysts, respectively. It is seen to be proportional to the number of Brønsted acid sites for HNaY as well as for USY zeolites. This confirms that the hydrogenation of eth-

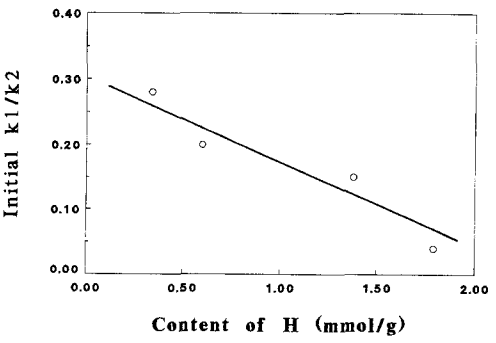

FIG. 10. Relationship between the initial k_1/k_2 at 723 K and the proton content in USY catalysts.

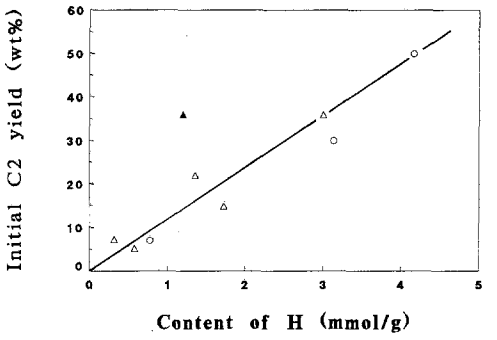

FIG. 11. Relationship between the initial ethane yield at 723 K and the proton of the zeolites: (○) HNaY, (△) USY, (▲) NaUSY(8).

ylene at 723 K over these zeolites can be attributed to Brønsted acid sites.

Barthomeuf and Beaumont (*14*) reported that in a HY zeolite, acid sites with strengths higher than 88% of H_2SO_4 appear only when the degree of proton for sodium exchange is higher than 30%. The number of such strong acid sites increases further with the degree of sodium exchange. These authors found that the activity for isooctane cracking increased with the number of strong acid sites. Wachter (*17*) later advanced a more detailed interpretation of Brønsted site strength based on the available number of next-nearest-neighbor Al atoms.

On the other hand, Lunsford and coworkers, when studying methanol dehydration, cumene dealkylation (*15*), and hexane cracking (*16*), reported that compared to dealuminated HY, a normal HY was much less active than expected on the basis of the number of protonic sites present and concluded that the acidity of the proton is lower in the latter case.

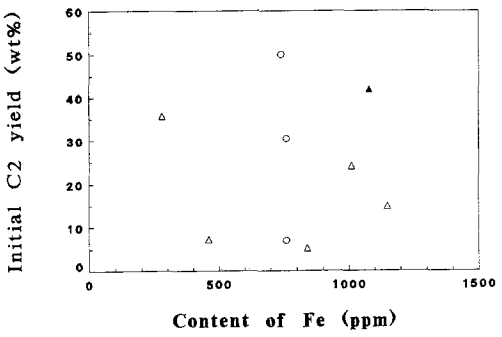

FIG. 12. Relationship between the initial ethane yield at 723 and the iron content of the zeolite samples: (○) HNaY, (△) USY, (▲) NaUSY(8).

In the present work, the initial yield of ethane over normal HY zeolites (HNaY) was higher than that over dealuminated Y zeolites (USY) and increased further with the degree of sodium ion exchange of HNaY, which is in agreement with the results of Barthomeuf and Beaumont (*14*). Therefore, it is concluded that: (i) strong acid sites are responsible for the hydrogenation of ethylene at 723 K, and (ii) such acid sites in HNaY and USY zeolites have comparable turnover numbers for the ethylene hydrogenation reaction (Fig. 11). Although the data at high yields strictly do not allow us to determine correct turnovers, the figure contains enough data that justify this general statement. On the other hand, the observed difference in yield of C_3 to C_5 alkanes over HNaY and USY zeolites can be attributed to the difference in the average acidity of the zeolites, assuming that the cracking reactions of ethylene oligomers require stronger acid sites than those available in HNaY.

Sano *et al.* (*7*) reported that HY zeolite shows a very low activity for the hydrocracking of benzene. This contradicts our observation that HNaY zeolites have a high activity for the hydrogenation of ethylene and our conclusion that such materials should have strong acidity. Several factors may explain this discrepancy. Either the activation of benzene or the cracking of cyclohexane, which is an intermediate product in the hydrocracking of benzene, demands even stronger acid sites than those needed for the hydrogenation of ethylene. Alternatively, since the deactivation of the normal HY zeolite is very fast, Sano *et al.* may have overlooked the initial high activity.

When the hydrogenation of ethylene over the USY catalysts was performed at a reac-

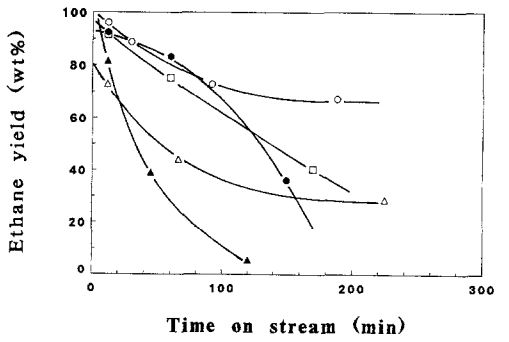

FIG. 13. Change of the ethane yield with time-on-stream at 623 K: (○) USY(4), (△) USY(8), (□) USY(11), (●) USY(27), (▲) USY(47).

tion temperature of 623 K, the main reaction product was ethane, the yield of methane and C_3 to C_5 hydrocarbons being below 10 wt%. The coke content of the used USY zeolites was below 2 wt%, indicating that the formation of ethane should be attributed to hydrogenation of ethylene rather than to hydrogen transfer reactions from coke to ethylene.

The ethane yield over USY catalysts is shown as a function of time-on-stream in Fig. 13. Despite the very low sodium content of the USY catalysts, the initial ethane yield on these catalysts is high and comparable to that obtained under the same conditions on HNaY-19 (Fig. 1). The iron content of USY(4) and USY(47) is lower than that of the HNaY samples (Table 2), so a major contribution from these sites is not to be expected.

The initial ethane yield from ethylene in the presence of hydrogen changes like temperature on HNaY-71 and USY(11). The yield first decreases, then increases with temperature (Fig. 14). Apparently, two types of sites exist: at low temperatures Na cations seem to be involved, at higher temperatures protons could be the active sites. Other arguments in line with such an assignment have already been advanced in the first section of this discussion.

For the hydrogenation of ethylene over NaUSY(8) at 723 K, the ethane yield was 35 wt% and exceeds the value predicted in Fig. 11. Moreover, between 703 and 723 K, the initial ethane yield decreases with increasing temperature (Fig. 14), in contrast to what happens on USY(11) and HNaY-71. These data suggest that on NaUSY(8), ethane comes to a large extent from the hydrogenation of ethylene on sodium cations even at 723 K. The ratio of the rate constants for ethane formation on NaUSY(8) and USY(8) is calculated to be 11.4 at 623 K, while the ratio of the sodium ions in the corresponding zeolites is 11.7. This suggests again that sodium cations are responsible for the hydrogenation of ethylene at 623 K over the USY catalysts. When at 623 K the turnover number for ethane formation on sodium cations is compared, it is found to be 35 times higher on NaUSY(8) compared with HNaY-19. Minachev *et al.* (*5*) calculated that the heats of heterolytic dissociation of hydrogen are highly exothermic and proposed that a heterolytic dissociative adsorption of hydrogen occurs on the cationic forms of zeolites ($Z–O^-$) in the following way:

$$Na^+ {}^-O–Z + H_2 \rightarrow Na^+ {}^-H + H^+ {}^-O–Z.$$

Thus it is proposed that hydrogenation over Na^+ occurs via consecutive addition of H ions to the double bond. Moreover, calculations show that hydride ion transfer is less endothermic than proton transfer (*5*). The

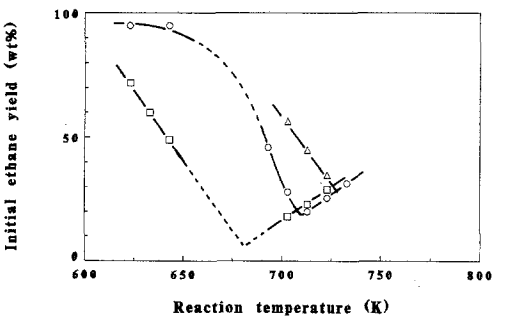

FIG. 14. Change of the initial ethane yield with reaction temperature, using 1 MPa of hydrogen: (○) USY(11), (△) NaUSY(8), (□) HNaY-71.

latter is, therefore, expected to occur faster on zeolites with stronger acid sites.

Rationalization of Zeolite Behavior in Ethylene Hydrogenation

The reaction order in hydrogen for ethylene hydrogenation was determined for HNaY-19 at 623 K and for hydrogen pressures ranging from 0.25 to 1 MPa. It has been shown earlier that Na^+ ions are active sites for such catalysts and reaction conditions. For USY(47) it was determined at 723 K for hydrogen pressures between 0.7 and 1.5 MPa. The active sites are now strong Brønsted acid sites. A first order in hydrogen was found for both reactions. This indicates that both hydrogenation of ethylene over sodium cations or Brønsted acid sites are first order in hydrogen. H_2–D_2 equilibration over iron impurities in Zeolite Y at a temperature of 673 K and a pressure of 5 kPa was found to be zero order in hydrogen (*1*). At higher hydrogen pressures and otherwise identical conditions, the activation of hydrogen should remain zero order in hydrogen. Therefore, in the present case, it seems unlikely that iron impurities are active sites. Thus, it is suggested that different hydrogenation mechanisms are active on the same catalyst, depending on the experimental conditions. This is summarized in Fig. 15. At low hydrogen pressures, hydrogen is activated on iron impurities in the zeolites. At high hydrogen pressures, the nature of the active site is temperature dependent. At low temperatures, residual alkali cations are active, while at higher temperature, strong Brønsted acid sites are involved.

Mechanism for the Hydrogenation of Ethylene over Brønsted Acid Sites in Faujasites

If ethane is formed by hydrogen transfer from coke to ethylene on Brønsted acid sites, hydrogen should be supplied by coke precursors. When deuterium is used instead of hydrogen in this reaction, the mechanism for the formation of ethane can be unravelled by detailed analysis of the tracer distribution in the reaction products. Furthermore, some information on the location of the rate-limiting step could be obtained by investigation of the existence of an isotopic effect in the formation of ethane.

The hydrogenation reaction of ethylene with deuterium was performed on USY(4) and USY(47) at a reaction temperature of 723 K. From the preceding discussion, it is likely that Brønsted acid sites are active. A comparison of the hydrogenation and deuteration reactions of ethylene on USY(4) and USY(47) is shown in Table 3. On both catalysts, the conversion and product distribution in the reaction was the same, whether H_2 or D_2 was used. Consequently, no isotopic effect is present.

GC/MS analysis of the reaction products from the ethylene deuteration reaction over USY(4) is shown in Fig. 16. Peak I must be attributed to C_2H_4 ($M = 28$). In the mass spectrum of peak II, the intense ions are separated by 2 mass units. Peak II should, therefore, be assigned to C_2D_4 rather than to $C_2H_4D_2$. The intense masses of peak III differ again by 2 mass units, its assignment to C_2D_6 being obvious. A minor contribution of $C_2H_{6-n}D_n$ ($n = 4, 5$) species cannot be excluded.

In peak IV, it seems that the low-intensity lines at $M/e = 46, 49, 51$, and 52 are the parent peaks of $C_3H_6D_2$, $C_3H_3D_5$, C_3HD_7, and C_3D_8, respectively. The strong lines at M/e from 30 to 34 are the corresponding fragment peaks ($C_2H_{5-n}D_n^+$ ($n = 1 - 5$)). Thus peak IV can be assigned to propane, which consists of $C_3H_{8-n}D_n$ ($n = 2, 5, 7, 8$). In peak V, the strong lines at M/e from 46 to 50 seem to be the fragment peaks ($C_3H_{7-n}D_n^+$ ($n = 3 - 7$)) of $C_4H_{10-n}D_n$ ($n = 3 - 10$). Thus peak V can be attributed to butane, consisting of $C_4H_{10-n}D_n$ ($n = 3 - 10$).

The considerable D incorporation in each saturated product, which is not significantly different for each of the alkanes, indicates that: (i) ethane is formed rather by cracking and hydrogen transfer as is the case for C_3

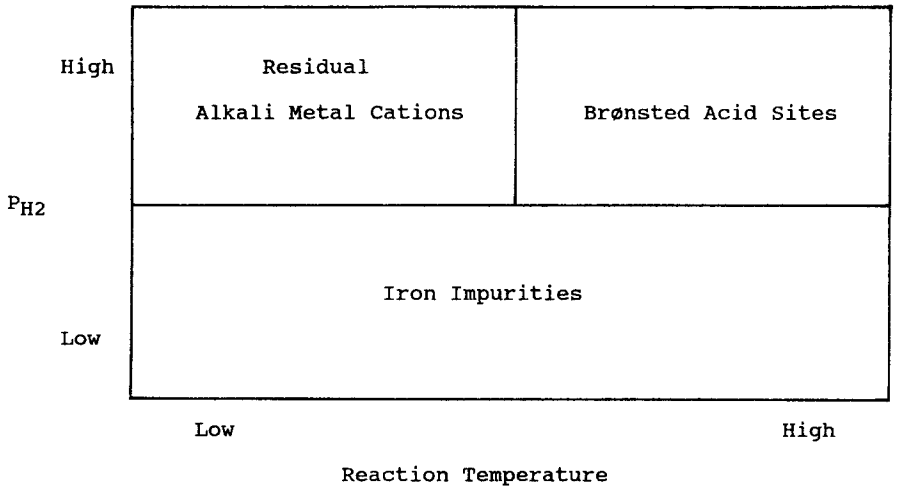

FIG. 15. Hydrogenation mechanisms of ethylene in metal-free zeolites.

and C_4 alkanes, and (ii) under the conditions of such hydrogen transfer, isotope scrambling is fast and abundant. It follows that the deuterium exchange of surface OH groups from D_2 gas and the deuterium incorporation in the substrate via surface OD groups is also fast. This is confirmed by the fact that peak II consists for a major part of deuterated ethylene. The exchange of surface OH groups with deuterium gas has been reported for acid zeolites (*18*).

TABLE 3

Comparison of the Reactions of Ethylene with Hydrogen or Deuterium over USY(4) and USY(47)[a]

Catalyst:	USY(4)		USY(47)	
Feed gas:	H_2	D_2	H_2	D_2
Ethylene conversion (wt%):	55.9	55.9	9.2	8.7
Selectivity (wt%)				
Methane	2.5	1.5	2.3	2.2
Ethane	25.8	23.0	79.3	80.1
Propylene	3.9	4.4	7.5	9.2
Propane	19.6	17.4	0.9	1.4
Butene	1.5	1.7	6.8	4.4
Butane	32.6	35.0	2.7	2.2
Pentene	0.1	0.1	0.0	0.0
Pentane	11.7	13.6	0.5	0.5
C_6^+ aliphatics	0.5	0.7	0.0	0.0
Aromatics	1.8	1.6	0.0	1.6

[a] 723 K, P_{H_2} or P_{D_2} = 1 MPa, $H_2(D_2):N_2:C_2H_4$ = 50:49:1, time-on-stream = 12 min.

In Fig. 17 the reaction products of the hydrogenation of ethylene with deuterium at 723 K over USY(47) are shown, together with the mass spectra of the respective peaks. The first peak consists of pure C_2H_4, while the second one shows a very typical mass spectrum. Low intensities are found at M/e = 31 and 32, while the lines at 30, 29, and 28 become increasingly important. This allows us to conclude that the M/e values of 31 and 32 represent parent peaks, while the masses at 28, 29, and 30 correspond to fragment peaks. It follows that in the second peak C_2H_5D and $C_2H_4D_2$ are the main components. However, the simultaneous presence of smaller amounts of C_2H_6 cannot be excluded. This confirms that ethane is formed by direct deuteration of ethylene on surface OH or OD groups.

It has already been suggested that the hydrogenation of ethylene on Brønsted acid sites is possible on a single surface site. Moreover, the selectivity for methane was very high in the hydrogenation reactions over the USY catalysts (Fig. 7). Therefore, it is proposed that the hydrogenation of ethylene via Brønsted acid sites is the reverse

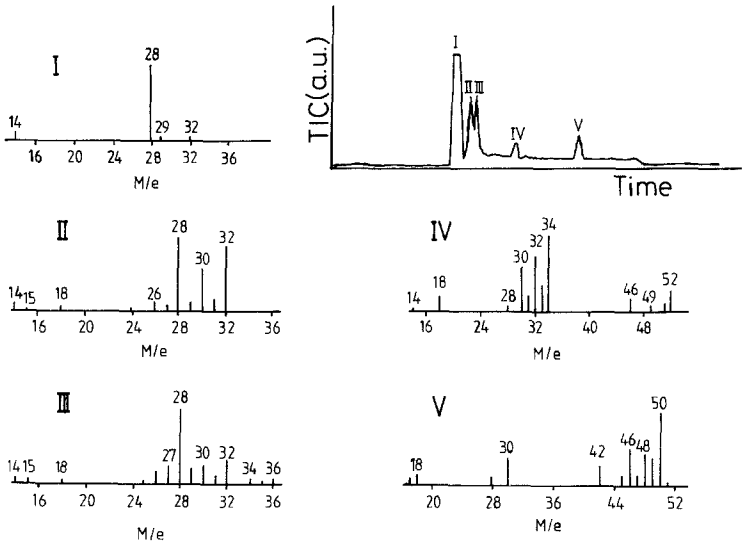

FIG. 16. Total ion chromatogram (TIC) in arbitrary units (a.u.) and corresponding mass spectra of each peak in the chromatogram, for the $D_2 + C_2H_4$ reaction at 723 K over USY(4).

reaction of the high-temperature pentacoordinated carbonium ion mechanism proposed by Haag and Dessau (*19*) in the reaction of alkanes over ZSM-5:

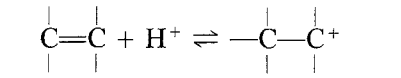

(I)

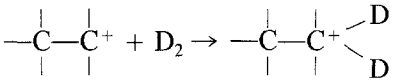

(II)

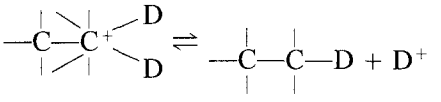

(IIIa)

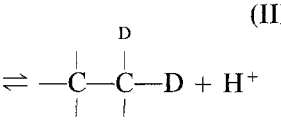

(IIIb)

This mechanism should explain (i) the first order in hydrogen, (ii) the absence of a major isotope effect, and (iii) the preferential formation of C_2H_5D and $C_2H_4D_2$. Equation (I)

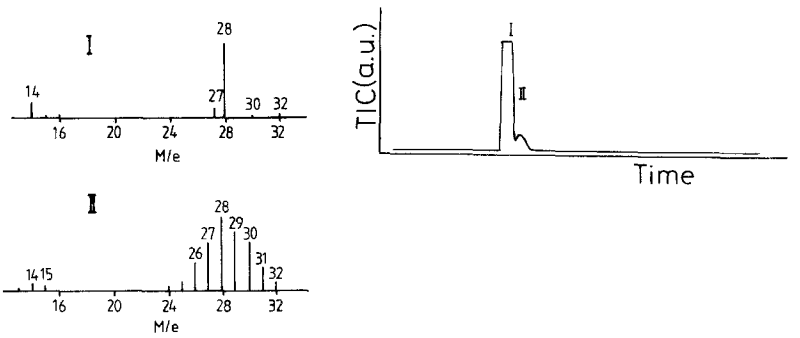

FIG. 17. Total ion chromatogram (TIC) in arbitrary units (a.u.) and corresponding mass spectra of each peak in the chromatogram, for the $D_2 + C_2H_4$ reaction at 723 K over USY(47).

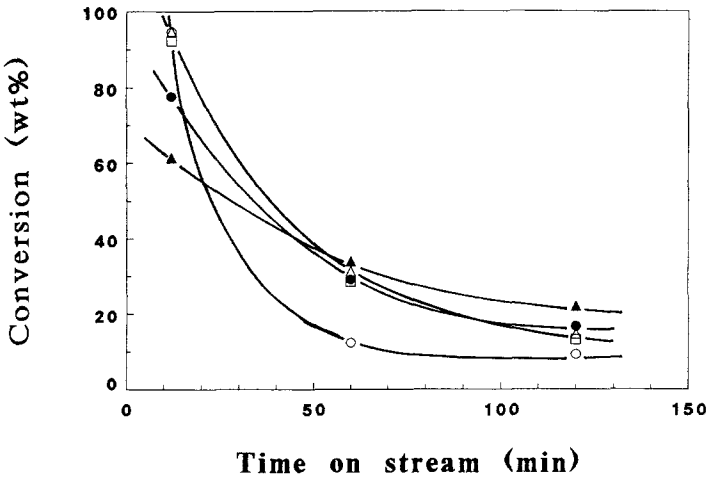

FIG. 18. Conversion of ethylene at 723 K in the presence of hydrogen as a function of time-on-stream over mordenite catalysts: (○) M(8), (△) M(11.1), (□) M(11.4), (●) M(23), (▲) M(49).

represents the protonation of an olefin and formation of a carbenium ion, which is fast and in no case rate determining. The transformation of a carbonium to the corresponding carbenium ion (reverse of Eq. (II)) is well documented (*20*). MO calculations predict that an ethyl carbonium ion can be viewed as a σ complex between the ethyl carbenium ion and hydrogen (IIa), or as a species with a three-center bond (IIb) or as a species with five full bonds, containing only eight electrons (IIc), which in its turn can also be regarded as a σ complex between ethane and H^+ (IId) (*21*).

$$CH_3CH_2^+ + H_2 \rightarrow CH_3CH_2^+ \leftarrow \begin{matrix} H \\ | \\ H \end{matrix} \equiv \quad \text{(IIa)}$$

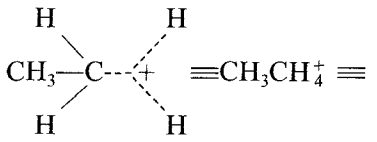

(IIb)

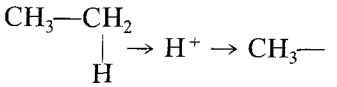

(IIc)

$$CH_3 + H^+ \quad \text{(IId)}$$

Although one deals with charged species, the conversion of a carbenium ion to a carbonium ion occurs in a concerted way as far as bond breaking of hydrogen is concerned and consequently does not require the existence of a large isotope effect. Such a concerted mechanism explains the lack of fast exchange of surface OD groups with the carbonium ion and the absence of heavily deuterated ethane.

Methane is then produced as follows:

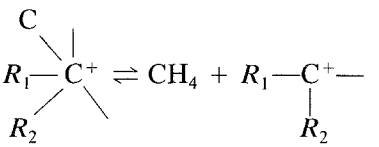

The formation of methane from larger alkylcarbonium ions will be preferred because of the higher stability of the larger alkylcarbenium ions formed. Since oligomerization of ethylene is a bimolecular reaction and should be enhanced by a higher acid density of the OH groups in the zeolite, the selectivity for methane would increase with decreasing Si/Al ratio of the zeolite. On the other hand, on a USY zeolite with a very high acid density, hydrogen transfer reactions will be preferred and the selectivity for methane reduced. The results of Fig. 7 agree with these trends.

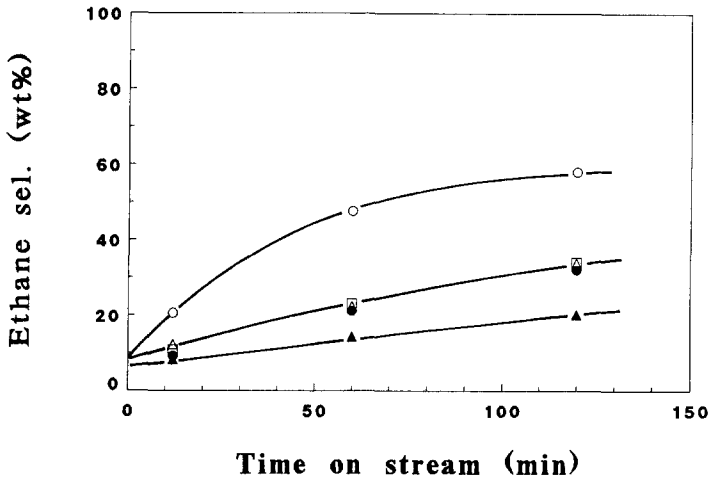

FIG. 19. Selectivity for ethane as a function of time-on-stream at 723 K: (○) M(8), (△) M(11.1), (□) M(11.4), (●) M(23), (▲) M(49).

Hydrogenation Activity on H-Mordenites (HM)

The hydrogenation of ethylene over HM catalysts was performed at a reaction temperature of 723 K. The variation of the ethylene conversion with time-on-stream is given in Fig. 18. The initial activity of these catalysts is lower for samples with lower aluminum contents, indicating that Brønsted acid sites are responsible for the catalytic activity. The selectivity for ethane and C_3 to C_5 alkanes of HM catalysts at 723 K is shown as a function of time-on-stream in Figs. 19 and 20, respectively. In all the experiments with HM catalysts, the initial ethane selectivity was very low and that of C_3 to C_5 alkanes was very high. After a time-on-stream of 2 h the coke content of used HM catalysts was about 8 wt%. The initial k_1/k_2

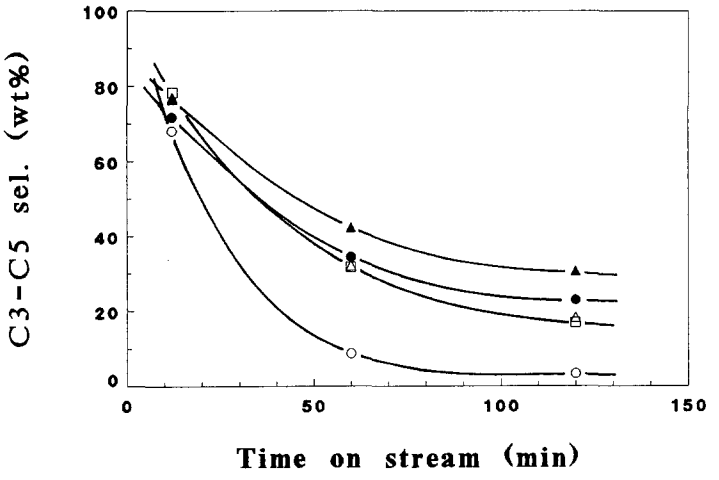

FIG. 20. Selectivity for C_3–C_5 alkanes as a function of time-on-stream at 723 K: (○) M(8), (△) M(11.1), (□) M(11.4), (●) M(23), (▲) M(49).

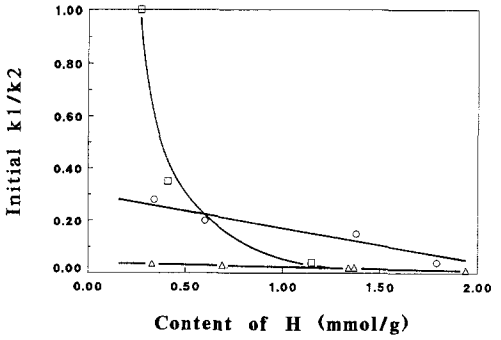

FIG. 21. Relationship between the initial k_1/k_2 at 723 K and the proton content: (○) USY, (△) M, (□) ZSM-5.

parameters of HM catalysts are lower than those of USY catalysts and do not change with the proton content (Fig. 21). These data suggest that on all HM catalysts, hydrogen transfer reactions are dominant at 723 K. Hydrogen transfer needs strong acid sites and a high acid density. Then the high rate of formation of C_3 to C_5 alkanes can be attributed to a strong acidity and the high topological acid density of the mordenite framework (*22*). Bodart *et al.* (*23*) proposed that even after dealumination, in HM paired Al sites are preferred.

Hydrogenation Activity on HZSM-5

The hydrogenation of ethylene on HZSM-5 catalysts was also performed at a reaction temperature of 723 K. In all the experiments, the conversion of ethylene was higher than 90 wt% and the main products were C_1 to C_5 alkanes. As shown in Figs. 21 and 22, the initial k_1/k_2 parameter and the selectivity for ethane on ZSM-5(60) were higher than those of HZSM-5(13) and HZSM-5(39).

After a time-on-stream of 5 h the coke content of used HZSM-5 was below 0.1 wt%. This low coke formation on HZSM-5 has been accounted for by steric factors (*24*). It seems that on HZSM-5 catalysts, C_2 to C_5 alkanes to a large extent come from true hydrogenation of C_2 to C_5 alkenes. Since the iron and sodium content of HZSM-5 catalysts is low (Table 2), it is suggested that acid sites of these catalysts are responsible for the hydrogenation of C_2 to C_5 alkenes. The high rate of formation of C_2 to C_5 alkanes by hydrogenation over HZSM-5 agrees with the results of Sano *et al.* (*6*).

HZSM-5(60) shows a higher initial yield of ethane than HNaY and USY catalysts, suggesting that Brønsted acid sites of ZSM-5(60) have a higher turnover number for ethane formation than HNaY and USY catalysts. Wielers *et al.* (*25*) have shown that protolytic cracking via carbonium ions becomes more pronounced with decreasing pore dimensions of the zeolite and have attributed it to transition state shape selectivity. Therefore, the higher initial ethane yield and k_1/k_2 parameter obtained with HZSM-5(60), compared to faujasites and mordenites (Fig. 21), can be associated with the same shape-selective effect, as the hydrogenation reaction is the reverse of the protolytic cracking.

HZSM-5(13) and HZSM-5(39) showed a low selectivity for ethane and a low initial k_1/k_2 parameter (Figs. 21 and 22). Since on these catalysts C_3 to C_5 alkanes seem to be produced by hydrogenation of C_3 to C_5 alkenes, this can be attributed to a high rate of ethylene oligomerization, which should be enhanced by the higher acid site density in these zeolites. On the other hand, the low

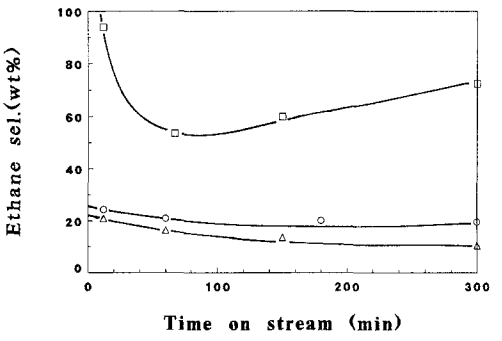

FIG. 22. Selectivity for ethane as a function of time-on-stream at 723 K: (○) ZSM-5(13), (△) ZSM-5(39), (□) ZSM-5(60).

initial k_1/k_2 could be due to the secondary formation of ethylene by cracking of C_3 to C_5 alkanes on these catalysts. Mole and Anderson (*26*) reported that cracking of propane is significant on HZSM-5 in the present conditions.

CONCLUSIONS

Several hypotheses on the nature of the sites responsible for the activation of hydrogen in metal-free zeolites have been advanced in the past. These discrepancies have not yet been rationalized. In the present work, it is proposed that different active sites can be operative on the same catalyst, the contribution of the different mechanisms depending on the reaction temperature and the hydrogen partial pressure.

At a relatively high hydrogen pressure, it is shown that the active sites responsible for the hydrogenation of ethylene change from sodium cations to Brønsted acid sites when the reaction temperature is increased. It is suggested that the hydrogenation of ethylene on Brønsted acid sites is a concerted reaction, occurring via a mechanism in which the hydrogenation of ethyl carbenium ion into the corresponding carbonium ion is the key step.

ACKNOWLEDGMENTS

J.A.M. acknowledges the support of the Belgian National Fund for Scientific Research for a fellowship as Research Associate. This research was sponsored partly by the Belgian Ministry of Scientific Affairs (GOA) and partly by NFWO-FNRS. J.K. acknowledges an overseas sabbatical stay from Idemitsu Kosan and financial support for the stay from the Japan Cooperation Center for Petroleum Industry Development (JCCP).

REFERENCES

1. Heylen, C. F., Jacobs, P. A., and Uytterhoeven, J. B., *J. Catal.* **43,** 99 (1976).
2. Jacobs, P. A., and Uytterhoeven, J. B., *J. Catal.* **50,** 109 (1977).
3. Gnep, N. S., Martin de Armando, M. L., Marcilly, C., Ha, B. H., and Guisnet, M., *in* "Catalyst Deactivation" (B. Delmon and G. F. Froment, Eds.), Studies in Surface Science and Catalysis, Vol. 6, p. 79. Elsevier, Amsterdam, 1980.
4. Minachev, Kh. M., Garanin, V. I., Kharlamov, V. V., and Isakova, T. A., *Kinet. Katal.* **13,** 1101 (1972).
5. Minachev, Kh. M., Kharlamov, V. V., Garanin, V. I., and Zelinsky, N. D., *in* "Catalysis on Zeolites" (D. Kalló and Kh. M. Minachev, Eds.), p. 489. Akadémiai Kiadó, Budapest, 1988.
6. Sano, T., Hagiwara, H., Okabe, K., Okado, H., Saito, K., and Takaya, H., *Sekiyu Gakkaishi* **29,** 89 (1986).
7. Sano, T., Shoji, H., Okabe, K., Saito, K., Hagiwara, H., Hosoya, T., and Takaya, H., *Sekiyu Gakkaishi* **29,** 257 (1986).
8. Tissler, A., Polanek, P., Girrbach, U., Muller, U., and Unger, K. K., *in* "Zeolites as Catalysts, Sorbents and Detergent Builders" (H. G. Karge and J. Weitkamp, Eds.), Studies in Surface Science and Catalysis, Vol. 46, p. 399. Elsevier, Amsterdam, 1989.
9. Jacobs, P. A., and Martens, J. A., Eds., "Synthesis of High-Silica Aluminosilicate Zeolites," Studies in Surface Science and Catalysis, Vol. 33, pp. 19 (10a). Elsevier, Amsterdam, 1989.
10. zur Strassen, H., *Z. Phys. Chem. (Leipzig) A* **169,** 81 (1934).
11. Pine, L. A., Maher, P. J., and Wachter, W. A., *J. Catal.* **85,** 466 (1984).
12. Guisnet, M., Avendano, F., Bearez, C., and Chevalier, F., *J. Chem. Soc., Chem. Commun.*, 336 (1985).
13. Giannetto, G., Sansare, S., and Guisnet, M., *J. Chem. Soc., Chem. Commun.*, 1302 (1986).
14. Barthomeuf, D., and Beaumont, R., *J. Catal.* **30,** 288 (1973).
15. DeCanio, S. J., Sohn, J. R., Fritz, P. O., and Lunsford, J. H., *J. Catal.* **101,** 132 (1986).
16. Sohn, J. R., DeCanio, S. J., Fritz, P. O., and Lunsford, J. H., *J. Phys. Chem.* **90,** 4847 (1986).
17. Wachter, W. A., *in* "Theoretical Aspects of Heterogenous Catalysis" (J. B. Moffat, Ed.), pp. 128–130. Van Nostrand–Reinhold, New York, 1989.
18. Heylen, C. F., and Jacobs, P. A., *Adv. Chem. Ser.* **121,** 490 (1973).
19. Haag, W. O., and Dessau, R. M., *in* "Proceedings, 8th International Congress on Catalysis, Berlin, 1984," Vol. 2, p. 305. Dechema, Frankfurt-am-Main, 1984.
20. For a review see Martens, J. A., and Jacobs, P. A., *in* "Theoretical Aspects of Heterogenous Catalysis" (J. B. Moffat, Ed.), Chap. 2. Van Nostrand–Reinhold, New York, 1989.
21. Vogel, P., *in* "Carbocation Chemistry," pp. 62, 63. Elsevier, Amsterdam, 1985.
22. Barthomeuf, D., *Mater. Chem. Phys.* **17,** 49 (1987).

23. Bodart, P., B. Nagy, J., Debras, G., Gabelica, Z., and Jacobs, P. A., *J. Phys. Chem.* **90,** 5183 (1986).
24. Rollman, L. D., and Walsh, D. E., *J. Catal.* **56,** 139 (1979).
25. Wielers, A. F. H., Vaarkamp, M., and Post, M. F. M., *J. Catal.* **127,** 51 (1991).
26. Mole, T., and Anderson, J. R., *Appl. Catal.* **17,** 141 (1985).